Eurographics Workshop on Visual Computing for Biology and Medicine (2015)
K. Bühler, L. Linsen, and N. W. John (Editors)

Image registration methods for patient-specific virtual physiological human models

J. E. E. de Oliveira[1] and P. Giessler[1] and T. M. Deserno[1]

[1]Department of Medical Informatics, Uniklinik RWTH University Aachen, Germany

Abstract

In this paper, current status of image registration is reviewed with respect to physiological, morphological and anatomical aspects. There are ample choices of recent techniques for image registration which can be used, and a technique suitable for image registration of the pelvis region supporting the femoral nerve block was applied for the development of patient-specific models. Virtual physiological human (VPH) model and magnetic resonance image (MRI) are used for patient-specific image registration. Results are presented in the form of image registration with respect to the skin of the models.

Categories and Subject Descriptors (according to ACM CCS): I.4.3 [Image Processing and Computer Vision]: Registration—

1. Introduction

Anatomical models are used in medical simulations to improve the diagnosis and assist the physician. In medical studies based on anatomical modelling, it is a general interest to analyze more than one data set simultaneously, and images obtained with different acquisition technologies can reveal additional information on structures of interest to an application. This can be achieved by image registration which is the process of aligning two or more images with the goal to find the optimal transformation that best aligns the structures of interest in the input images [Roh00, ZF03].

Medical image registration can unify image information from different anatomical modalities [MV98, HBHH01, OT14] such as magnetic resonance images (MRI), computed tomography (CT), X-ray, and ultrasound (US). Anatomical image registration, in the medical field, is a key component in several areas like diagnosis and image guidance [HRG*09, UNS*13], radiation therapy [FCC*11, FBB*14], biopsy [YAHF11], and surgical planning [HCLD13, GHM*15].

The state of art of anatomical modeling is enhanced by fitting automatically relevant patient data into virtual physiological humans (VPH) template models to generate patient-specific training modules, instead of relying on generic models. Through an integration of image processing, physiological models, subject-specific data, and virtual reality, the Regional Anaesthesia Simulator and Assistant (RASimAs) project aims at developing a training simulator and assistant prototype for regional anaesthesia (RA) procedures which will increase the application, the effectiveness, and the success rates of RA by combining a simulator and assistant supporting ultrasound-guided RA and electrical nerve-stimulated RA [DdOG15].

The performance of regional anaesthesia necessitates blocking the peripheral nerves by local injection of anaesthesia, and it is a technique which demands training and assistance. RA has several advantages in comparison with general anaesthesia (GA):

- For the patient: no loss of consciousness, no risk of aspiration, less risk of postoperative nausea and vomiting and minimized probability for adverse drug reactions or allergy, less cardiovascular stress, and superior pain control after the surgery [GKEea09].
- For the society: shorter hospital stay and costs savings of 100.000 € per year per operation theater without compromising care [MHGKK10].

The femoral nerve block is performed on the pelvis region and creating anatomical VPH models for this region is

DOI: 10.2312/vcbm.20151206

challenging, as generic commercial VPH models may not be accurate and do not consider anatomical variations. One of the challenges is to find an existing image registration technique which considers individual patient anatomy and use general models to generate patient-specific computer models for application in RA procedures, applying image registration techniques for a mesh and voxel basis methods. In this paper, in the context of anatomical modeling, a survey is presented so that the existing techniques and toolkits are highlighted in a way that one of them is used for patient-specific image registration, in order to extract different tissue classes such as skin surface, muscle, fat, bone and nerves.

2. Material and Methods

2.1. Selection of the papers

Medical image registration papers were identified using a non-systematic search in Pubmed, Science Direct, IEEE Xplore Digital Library, and ACM Digital Library. The following search terms: 'anatomical', 'anatomic', 'image registration', 'techniques' were combined and subsequently, the search was performed in the identified sources published between 2008 and 2015.

Table 1 presents a summary of the surveyed papers.

2.2. Image Registration Methods

The criteria used in this paper for the review is to present (i) the goal of image registration, (ii) the anatomical region of interest, (iii) the image data, (iv) the applied technique.

Gilles et al. [GP08] applied shape matching in musculoskeletal MRI images for inter-patient registration. Elastic deformation is approximated by shape matching which works as a regularization step that filters out noise from external forces proposing a modified force-based evolution scheme. Non-rigid deformations are simulated by blending rigid transforms of overlapping clusters (which contains object vertices) of mesh regions.

With the aim of employing fused images during both diagnosis and image guidance for minimally invasive surgical procedures, Huang et al. [HRG*09] executed a registration of intra procedure US with pre procedure dynamic 3-D MR/CT images of the beating heart. A two-step mutual information (MI)-based registration method was proposed: (i) a initial manual registration which result is further refined using a MI-based registration method, and (ii) a intra procedure registration, which transforms the registration obtained in the preliminary step through the tracking transformation matrix to the new pose as a new starting point refined by a rapid MI technique.

Martin-Fernandez et al. [MFCMM*09] had the goal of helping medical doctors in the bone age assessment. Conventional X-ray images of the hand were used for the development of a new method called articulated registration. This method models the inner bone skeleton with a wire model, where wires are drawn by connecting landmarks located in the main joints of the skeletal structure to be registered (long bones). The registration on long bones is affine meanwhile the registration of soft tissues (far from the bones) is elastic.

Scheys et al. [SLS*09], regarding the musculoskeletal system, had the aim to estimate a subject's musculoskeletal geometry with the information extracted from MRI images. A novel method using non-rigid image registration was reported which is obtained through two steps: (i) automated rigid or affine registration, and (ii) a non-rigid intensity based registration. As a similarity measure, MI was used.

Also working with musculoskeletal system and extending a previous work, Gilles et al. [GMT10] proposed a new framework for image segmentation and registration of MRI images. The approach is based on discrete deformable surfaces and the introduction of scalable simplex surfaces equipped with reversible medial representations. Different issues were considered in the process: the initial construction and adaptation of generic models, the computation of relevant internal and external constraints and the model evolution.

King et al. [KRM*10] had the goal of providing valuable anatomical information of the heart for image-guided interventions. A novel technique for computing the image-to-physical registration for minimally invasive cardiac interventions is presented using MRI and US heart images. First, the technique uses an automatic cardiac segmentation tool which is augmented with knowledge of the acoustic properties of different tissue regions (i.e., blood and muscle). The augmented segmentation is transformed by two transformations: the rigid registration, which aligns the MRI and 3-D US coordinate systems, followed by the affine respiratory motion correction transformation, which corrects for any breathing motion.

Establishing the spatial extent of prostate cancer on radiological imaging was the purpose of the work of Chappelow et al. [CBR*11]. Prostate MRI images with corresponding whole-mount histology (WMH) sections were registered using a method for automated elastic registration which was called multiattribute combined mutual information (MACMI). MACMI allows for incorporation of multiple modalities, protocols, or even feature images in an automated registration scheme, facilitated by the use of multivariate MI.

The detection of lung deformations during and following radiotherapy was in the scope of Faggiano et al. [FCC*11]. Planning kilovoltage CT (kVCT) images and mega voltage CT (MVCT) images of the lung parenchyma were elastically registered using a method based on free-form deformation and MI. First, a pre processing step was performed to deal with differences in images extent. Registration was applied and the spatial transformation was modeled as a sum of a

Table 1: *Summary of anatomical image registration papers*

Paper	Goal	Anatomical Structure	Image data	Techniques	
				Algorithms	Nature of the registration basis
[GP08]	Inter-patient registration	Musculoskeletal	MRI - MRI	Shape matching	Surface
[HRG*09]	Diagnosis and image guidance	Heart	US - MRI/CT	Mutual information-based registration method	Voxel
[MFCMM*09]	Bone age assessment	Hands	X-ray - X-ray	Articulated registration	Surface
[SLS*09]	Estimation of geometry	Musculoskeletal	MRI - MRI	Non-rigid image registration and mutual information	Voxel
[GMT10]	Inter and intra-patient registration	Musculoskeletal	MRI - MRI	Simplex meshes	Voxel
[KRM*10]	Image-guided interventions	Heart	MRI - US	Rigid registration	Voxel
[CBR*11]	Establish extent of cancer	Prostate	MRI - WMH	Multiattribute combined mutual information	Voxel
[FCC*11]	Radiotherapy	Lung parenchyma	MVCT - kVCT	Free-form deformation and mutual information	Voxel and Surface
[LCP*11]	Radiotherapy	Pelvis	MRI - MRI (cervical cancer) and CBCT - CBCT (prostate cancer)	Non-rigid registration based on multi-resolution cubic B-spline and FFD	Surface
[YAHF11]	Biopsy	Prostate and Neck	PET/CT - TRUS	Combination of point-based registration and volume matching method	Surface
[LSU*12]	Technique development	Brain	MRI - Histological sections	Local curvature	Surface
[TMB12]	Assessment of bone fracture risk	Bone	microCT - microCT	Surface-based registration technique	Surface
[CLS*13]	Investigate and manage retinal pathology	Retina	OCT - OCT	Deformable image registration	Surface
[HCLD13]	Surgical planning	Bones	MRI - TP and X-ray	Articulated model and thin-plate spline	Surface
[SD13]	Therapy guidance	Left atrium and pulmonary veins	CT - US	Intensity-based similarity measures	Voxel
[UNS*13]	Guidance for surgery	Lung	CBCT - CBCT	Deformable image registration	Surface
[ZFF*13]	Radiotherapy	Pelvis	CT - CT and CT - CBCT	Deformable image registration	Surface
[FBB*14]	Radiotherapy	Pelvis	CT - CT and CT-CBCT	Varian Rigid Registration package (version 10.0)	Surface
[KYK*14]	Radiotherapy	Brain	CT - MRI	Ratio image uniformity and mutual information	Surface
[MvK14]	Radiotherapy	Head and neck	CBCT - pCT	Deformable image registration	Surface
[Spi14]	Image guided intervention	Abdomen	CT-CT	Rigid registration	Surface
[GHM*15]	Image guided evaluation	Elbow	3D CT - 2D fluoroscopic images	Weighted histogram of gradient directions of the image	
[HHH*15]	Radiotherapy	Lung	PET/CT - pCT	Rigid and deformable image registration	Surface
[KWW*15]	Augment performance	Brain	MRI - MRI	Deformable image registration	Surface
[RCC15]	Surgical resection	Brain	3D US - MRI	Robust patch-based correlation ratio	Voxel

global rigid transformation to correct the global misalignment and a local elastic deformation. Both transformations were estimated using the similarity measure of mutual information (MI).

With the pelvis as a region of interest, Lu et al. [LCP*11] planned to deliver high doses of radiation to cancerous regions while maintaining or lowering doses to surrounding non-cancerous regions. For cervical cancer, the registration was performed for MRI images, while for prostate cancer, registration was realized for cone-beam CT (CBCT) images. The model proposed was based on a Maximum A Posterior (MAP) framework while the automatic segmentation part extended a previous level set deformable model with shape prior information. The constrained nonrigid registration part was based on a multi-resolution cubic B-spline Free Form Deformation (FFD) transformation to capture the internal organ deformation.

Yang et al. [YAHF11] presented a 3D non-rigid algorithm with the aim of biopsy of the targeted prostate biopsy using in combining positron emission tomography(PET)/CT and transrectal ultrasound (TRUS) images. The registration method is a hybrid approach that simultaneously optimizes the similarities from point-based registration and volume matching methods and includes three terms: (1) surface landmark matching, (2) internal landmark matching, (3) volume overlap matching. The 3D registration is obtained by minimizing the distances of corresponding points at the surface and within the prostate and by maximizing the overlap ratio of the bladder neck on both images.

Liu et al. [LSU*12] developed a technique to automate landmark selection for nonlinear medical image registration using local curvature on anatomical contours applied to MRI and histological sections of brain images. Interpolating transformations were calculated from homologous point landmarks on the source (image to be transformed) and target (reference image). The MRI slices and histological sections were nonlinearly registered using the thin-plate splines with the landmarks generated and optimized by the presented technique.

For the assessment of bone fracture risk, microCT bone images were registered in the work of Tassani et al. [TMB12] applying a surface-based registration technique. This technique comprises the application of a segmentation process by means of a global fixed threshold, the definition of a measure of match (MOM) that quantifies the spatial matching between the pre and post failure sets, and a maximization of the MOM. The geometrical transformation employed was the rigid transformation model.

Investigating and managing the retinal pathology was the purpose of Chen et al. [CLS*13]. They proposed a new deformable registration algorithm for optical coherence tomography (OCT) images of the retina. A retinal OCT specific affine alignment (A-OCT) was performed by translating the foveae between the two images and then individually scaling each subject A-mode scan to match the corresponding target A-mode scan. Then, a deformable registration (D-OCT) in the A-mode direction was used to further align the retinal layers. Outside of the initial fovea alignment, the registration was performed by only comparing the similarity between pairs of A-mode scans.

Harmouche et al. [HCLD13], with the aim of aiding in surgical planning, used bone structures from thoracic and lumbar vertebral from MRI, surface topography (TP) and X-ray images to register using an articulated model and the soft tissue using a constrained thin-plate spline transform. First, the TP data was registered to the X-ray reconstruction by applying a thin-plate spline transform. Then, the goal was to transform each MRI voxel into the space of the 3D X-ray model, taking into account the non-rigid deformation following the posture change subject to the following constraints: first, the spine extracted from the MRI images had to be aligned with the X-ray spine model. Second, MRI data of the torso had to be contained within the TP volume, such that the contour of the torso on the MRI corresponded to the surface topography. In order to register each MRI slice such that the spine information extracted from MRI data and that extracted from X-ray data are aligned, an articulated model previously used to align 3D models of the spine obtained from both modalities was calculated which allowed the definition of the spine as a combination of local intervertebral transformations which can be obtained in a number of ways.

In order to guide high intensity focused ultrasound therapy in patients with atrial fibrillation, Sandoval et al. [SD13] evaluated eight intensity-based similarity measures (six using information from the histograms of the images and two using spatial information and intensity values) which are used in rigid and elastic registration techniques to align preoperative CT and transesophageal US images of the left atrium and the pulmonary veins.

Uneri et al. [UNS*13], in a way to localize the targeting of small tumors during surgery, proposed a deformable registration algorithm for application in CBCT image from the lungs. The algorithm is composed of two major stages: a model-driven stage based on image features (to identify the structures that drive coarse registration), followed by an image-driven stage based on image intensities and gradients (using an intensity-corrected Demons algorithm.)

Images from the pelvis for a CT image registration were used by Zambrano et al. [ZFF*13] for radiotherapy planning. The authors proposed a deformable image registration algorithm based on the method proposed by Sohn et al. [SBCea08], and refined the constraints imposed for the final deformation field calculation. The algorithm divides both source (moving) and target (fixed) images into sub-volumes called featurelets which, in the source images, was independently rigidly registered to its corresponding one in the target image using a 3-degrees of freedom (DoF) rigid registration

(RR) approach with three translational parameters as a result.

Fortin el al. [FBB*14] evaluated the clinical impact in tumor volume definition of lung and head/neck images using deformable registration of acquired PET/CT with planning CT images. A commercially available software, the Varian Rigid Registration package (version 10.0) was used to register the images in two steps: a rigid image registration followed by a deformable image registration.

Kisaki et al. [KYK*14], with the purpose of radiotherapy planning, performed image registration in brain CT and MRI images applying a global matching method based on the Levenberg-Marquardt algorithm (provides a solution of the nonlinear least squares minimization problem). The proposed method is composed of two main steps: coarse registration based on the minimization of ratio image uniformity (RIU) and fine registration based on the maximization of normalized mutual information.

Using a deformable registration algorithm, Mencarelli et al. [MvK14], for the purpose of radiation therapy, applied the technique in head and neck CBCT and planning CT images. The authors implemented a cubic B-spline deformable registration algorithm with rigidity and volume constraints driven by a correlation ration.

Spinczyk et al. [Spi14] used CT images from the abdomen to verify the correspondence between rigid registration fiducial registration error signal and breathing phase, which is useful for percutaneous abdomen interventions in cases, where only the 3D image is used to build the preoperative anatomical model. The proposed method allowed semi-automated rigid registration to establish the correspondence between the preoperative patient anatomical model and patient position.

Image guided evaluation of musculoskeletal disorders and surgeries was the aim of the work of Ghafurian et al. [GHM*15]. A weighted histogram of gradient directions was applied as an image feature to measure the similarity of the 3D CT digitally reconstructed radiographs (DRRs) and the 2D fluoroscopic images. The proposed method simplifies the computation by searching the parameter space (rotation and translation) sequentially rather than simultaneously.

Hardcastle et al. [HHH*15] used a rigid and deformable image registration of CT for a radiotherapy treatment planning scan. First, a pre deformable image registration and rigid registration were performed using the 3DSlicer software (http://www.slicer.org). The CT component of the PET-CT was rigidly (translation and rotation) registered to the planCT image using an automated algorithm with a Mattes Mutual Information cost function. The PET data was then registered using the same registration. Two commonly used deformable image registration algorithms were investigated, B-splines and Demons, as they represent different approaches.

Aiming at augmenting the performance of registering two images, Kim et al. [KWW*15] presented a novel patch-based initial deformation prediction framework applied to brain images from MRI. There are two stages in the proposed framework. In the training stage, a large number of training images are carefully registered to a selected template and a dense formation field for each training image is obtained. In the application stage, for registering a new subject image with the same selected template, thin-plate splines are used to interpolate a dense deformation filed, which is used as the initialization to allow the registration algorithm estimating the remaining small segment of deformations toward the template image.

Rivaz et al. [RCC15], for surgical resection of brain tumors, automatically register preoperative MRI, acquired a few days before the surgery, to post resection US, using robust patch-based correlation ratio (RaPTOR). It computes local correlation ratio (CR) values on small patches and adds the CR values to form a global cost function; RaPTOR estimates the similarity measure locally and is robust against outlier data.

Images from the same modality were the most used for image registration, and techniques such as OCT, microCT, MVCT, kVCT, CBCT were employed for 3D dimension image registration. Surface-based image registration relies on the accurate segmentation of anatomical structures in the images to be registered and overcame the voxel-based image registration. A summary of the cited image registration methods can be seen in Table 1.

2.3. Patient-specific anatomical modeling

The papers presented applied a number of techniques adapted to a certain anatomical region and type of images, presenting monomodal (images from same modality) and multimodal (images from different modality) image registration. Also, a mesh to mesh or voxel to voxel registration is the majority of the presented works where registration is performed mostly on images and not using VPH models.

Regarding the pelvis region for the support of the femoral nerve block, the technique from Gilles et al. [GP08, GMT10] which method uses common registration approaches damped by shape matching characteristics of the mesh has shown suitable for the anatomical modeling. As Gilles's non-rigid registration approach offers the possibility to register a 3D mesh-model/voxel-data combination on a target voxel space, it was adapted for the development of a method for semi-automatic registration of a general model data towards partial MRI image of a real patient.

Five steps are performed (Figure 1) to achieve the anatomical modeling.

Step 1: Select the general model (here: Zygote) and the patient data (here: MRI). Zygote [zyg] is a commercial

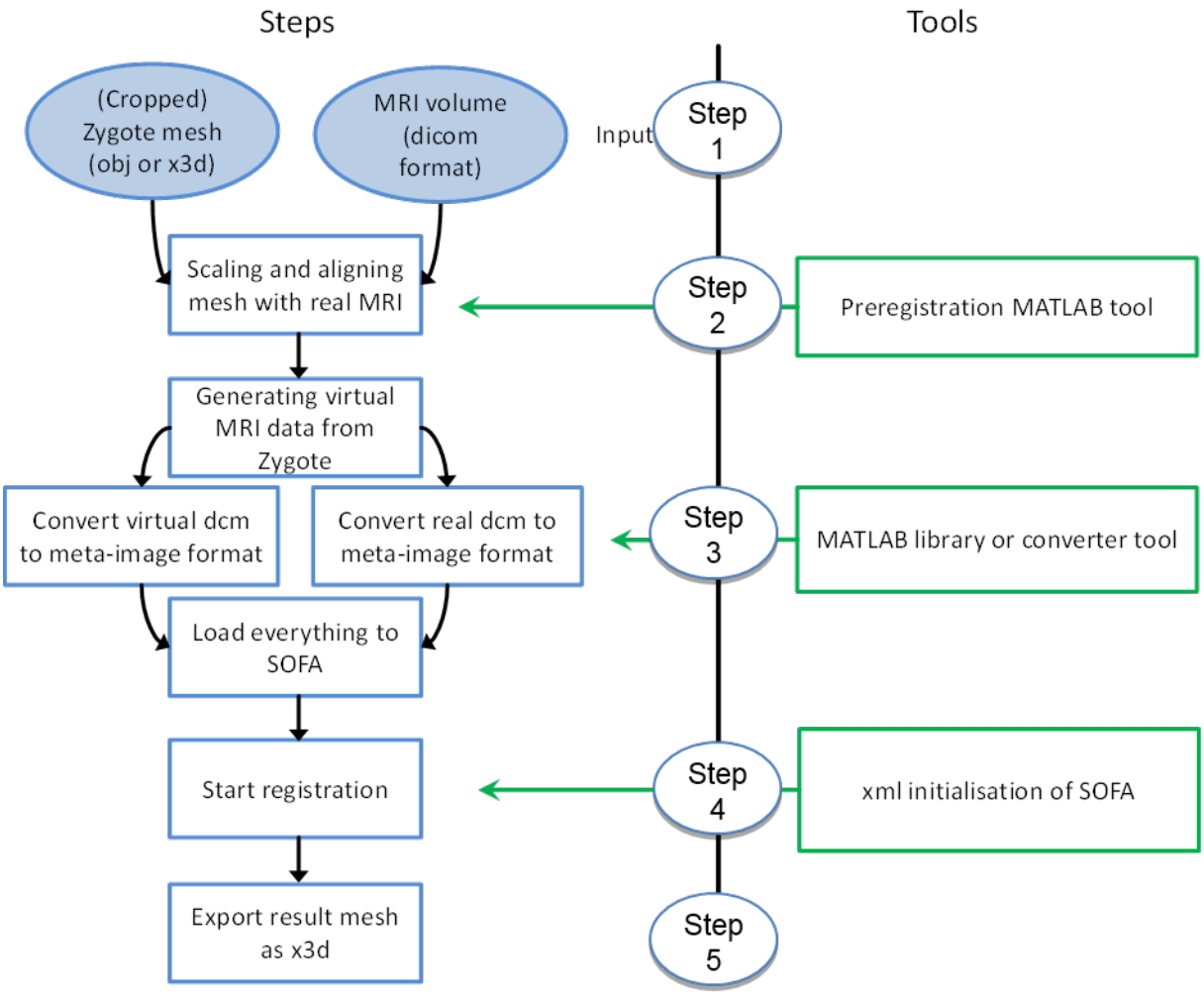

Figure 1: *Workflow for a mesh to voxel basis image registration*

dataset which yield the human anatomy in 3D and provide polygonal meshes, partly enhanced with texture. Patient data include MRI stored using Digital Imaging and Communications in Medicine (DICOM) standards.

Step 2: A pre-registration to create an initial alignment is manually defined by the user. Digitally reconstructed radiograph (DRR) are computed for both the virtual patient and for the DICOM images [SBLD15]. For the scaling and rigid alignment between mesh and MRI, a simple user interface has been created using MatLab and this tool creates frontal and lateral X-rays images of the mesh and the MRI data distinguishing among skin, muscle, and bones. From this rigid image registration process, a quaternion transformation matrix results, which is then applied to the cropped meshes.

Step 3: In this step, the technique presented by Gilles et al. [GP08, GMT10] is adapted and performed by means of SOFA [ACF*07]. A virtual MRI is generated based on the Zygote mesh. To set up intensity profiles, a step size s and the number of steps n that shall be taken in each direction is needed. For each vertex, there are n inwards and n outwards steps taken in each direction of the normal vector belonging to the vertex. Based on the normalized cross correlation between the reference and the target profiles, the algorithm calculates external forces for each vertex, i.e., it searches in a certain distance d, point which have the highest similarity value.

Step 4: For initialization, a reference volume of the mesh is needed, which is used to set up initial intensity profiles. Therefore, a virtual MRI of the Zygote mesh with generic gray intensity values for the four most important tissues of the MRI, i.e., fat, muscle, bone, air is created for the initialization of the algorithm of Gilles. Although there is a certain

lack of reality in this rough approach for virtual MRI generation, it turns out as sufficient for initialization purposes.

Step 5: The registered and deformed mesh model (here: Zygote) may be exported for further use.

3. Results and Discussion

Papers regarding anatomical image registration were presented and have shown several anatomical structures as the focus, such as brain, lung, prostate, bones, pelvis, and heart. The images were obtained from different modalities like CT, MRI, US and X-ray, and techniques from rigid and non-rigid image registration were applied for radiotherapy, image guidance, and surgical planning.

Among the present techniques and regarding the musculoskeletal system, one technique, from Gilles et al. [GP08, GMT10], was selected and used for a patient-specific modeling of the pelvis.

Examples of the resulting image registration are showed in Figures 2 and 4, considering two different subjects, a male and a female, respectively. These results can be visually compared with the male Zygote model in Figure 3 and the female Zygote model in Figure 5. Especially for the female on Figure 4, the personalization of the skin is highlighted, as this subject has more fat than the Zygote model.

The technique from Gilles et al. had to be adapted in order to work with a mesh to voxel image registration providing a new possibility for it, although only one surface per time can be registered. For now we presented the results regarding the skin, but the non-rigid image registration still has to be implemented for muscles and bones.

4. Conclusion

A review of anatomical image registration in the last few years was presented by showing the goal of the image registration, the anatomical structure and image data set with the applied techniques. A variety of techniques are used for different anatomical structures, making it a challenge to choose the best technique for a certain region.

For a patient-specific modeling for the pelvis, the technique from Gilles et al. was suitable for image registration and then applied to a commercial VPH model that was enhanced by incorporating patient data collected by MRI. Future works include a refined automatic registration of muscle and skeleton on MRI.

In summary, this review demonstrates that there is a wide selection of techniques that can be employed for a variety of anatomical image registration and the choice of one of them was adequate for patient-specific modeling of the pelvis region for the femoral nerve block.

Acknowledgment

This project has received funding from the European Union's Seventh Framework Programme for research, technological development and demonstration under grant agreement no 610425. We appreciate the detailed support by Benjamin Gilles providing us his SOFA implementations.

References

[ACF*07] ALLARD J., COTIN S., FAURE F., BENSOUSSAN P.-J., POYER F., DURIEZ C., DELINGETTE H., GRISONI L.: Sofa-an open source framework for medical simulation. In *MMVR 15-Medicine Meets Virtual Reality* (2007), vol. 125, IOP Press, pp. 13–18. 6

[CBR*11] CHAPPELOW J., BLOCH B. N., ROFSKY N., GENEGA E., LENKINSKI R., DEWOLF W., MADABHUSHI A.: Elastic registration of multimodal prostate MRI and histology via multiattribute combined mutual information. *Med Phys 38*, 4 (2011), 2005–18. 2, 3

[CLS*13] CHEN M., LANG A., SOTIRCHOS E., YING H. S., CALABRESI P. A., PRINCE J. L., CARASS A.: Deformable registration of macular OCT using Amode scan similarity. *Proc IEEE Int Symp Biomed Imaging* (2013), 476–79. 3, 4

[DdOG15] DESERNO T. M., DE OLIVEIRA J. E. E., GROTTKE O.: Regional anaesthesia simulator and assistant (RASimAs. *Proceedings of the 28th IEEE International Symposium on Computer-Based Medical Systems* (2015), 348–351. 1

[FBB*14] FORTIN D., BASRAN P. S., BERRANQ T., PETERSON D., WAI E. S.: Deformable versus rigid registration of PET CT images for radiation treatment planning of head and neck and lung cancer patients a retrospective dosimetric comparision. *Radiat Oncol 10* (2014), 50. 1, 3, 5

[FCC*11] FAGGIANO E., CATTANEO G. M., CIAVARRO C., DELL'OCA I., PERSANO D., CALANDRINO R., RIZZO G.: Validation of an elastic registration technique to estimate anatomical lung modification in non-small-cell lung cancer tomotherapy. *Radiat Oncol 6* (2011), 31. 1, 2, 3

[GHM*15] GHAFURIAN S., HACIHALILOGLU I., METAXAS D. N., TAN V., LI K.: 3D/2D image registration using weighted histogram of gradient directions. *Proc of SPIE 9415* (2015), 94151Z–1–7. 1, 3, 5

[GKEea09] GONANO C., KETTNER S. C., ERNSTBRUNNER M., ET AL: Comparison of economical aspects of interscalene brachial plexus blockade and general anaesthesia for arthroscopic shoulder surgery. *Br J Anaesth 103*, 3 (2009), 428–33. 1

[GMT10] GILLES B., MAGNENAT-THALMANN N.: Musculoskeletal MRI segmentation using multi-resolution simplex meshes with medial representations. *Med Image Anal 14*, 3 (2010), 291–302. 2, 3, 5, 6, 7

[GP08] GILLES B., PAI D. K.: Fast musculoskeletal registration based on shape matching. *Med Image Comput Comput Assist Interv 11*, Pt 2 (2008), 822–9. 2, 3, 5, 6, 7

[HBHH01] HILL D. L. G., BATCHELOR P. G., HOLDEN M., HAWKES D. J.: Medical image registration. *Phys Med Biol 46* (2001), R1–R45. 1

[HCLD13] HARMOUCHE R., CHERIET F., LABELLE H., DANSEREAU J.: Multimodal image registration of the scoliotic torso for surgical planning. *BMC Med Imaging 13* (2013), 1–12. 1, 3, 4

[HHH*15] HARDCASTLE N., HOFMAN M. S., HICKS R. J.,

CALLAHAN J., KRON T., MACMANUS M. P., BALL D. L., JACKSON P., SIVA S.: Accuracy and utility of deformable image registration in 68-ga 4D PET CT assessment of pulmonary perfusion changes during and after lung radiotherapy. *Int J Radiat Oncol Biol Phys In press* (2015). 3, 5

[HRG*09] HUANG X., REN J., GUIRAUDON G., BOUGHNER D., PETERS T. M.: Rapid dynamic image registration of the beating heart for diagnosis and surgical navigation. *IEEE Trans Med Imaging 28*, 11 (2009), 1802–14. 1, 2, 3

[KRM*10] KING A. P., RHODE K. S., MA Y., YAO C., JANSEN C., RAZAVI R., PENNEY G. P.: Registering preprocedure volumetric images with intraprocedure 3-D ultrasound using an ultrasound imaging model. *IEEE Trans Med Imaging 29*, 3 (2010), 924–37. 2, 3

[KWW*15] KIM M., WU G., WANG Q., LEE S. W., SHEN D.: Improved image registration by sparse patch-based deformation estimation. *Neuroimage 105* (2015), 257–68. 3, 5

[KYK*14] KISAKI M., YAMAMURA Y., KIM H., TAN J. K., ISHIKAWA S.: High speed image registration of head CT and MR images based on levenberg-marquardt algorithms. *Int Conf Soft Comput and Intell Syst* (2014), 1481–85. 3, 5

[LCP*11] LU C., CHELIKANI S., PAPADEMETRIS X., KNISELY J. P., MILOSEVIC M. F., CHEN Z., JAFFRAY D. A., STAIB L. H., DUNCAN J. S.: An integrated approach to segmentation and nonrigid registration for application in image-guided pelvic radiotherapy. *Med Image Anal 15*, 5 (2011), 772–85. 3, 4

[LSU*12] LIU Y., SAJJA B. R., UBERTI M. G., GENDELMAN H. E., KIELIAN T., BOSKA M. D.: Landmark optimization using local curvature for point based nonlinear rodent brain image registration. *Int J Biomed Imaging 2012* (2012), 1–8. 3, 4

[MFCMM*09] MARTIN-FERNANDEZ M. A., CARDENES R., MUNOZ-MORENO E., R. LUIZ-GARCIA M. M.-F., ALBEROLA-LOPEZ C.: Automatic articulated registration of hand radiograph. *Image Vis Comput 27* (2009), 1207–22. 2, 3

[MHGKK10] MARHOFER P., HARROP-GRIFFITHS W., KETTNER S., KIRCHMAIR L.: Fifteen years of ultrasound guidance in regional anaesthesia: part 1. *Br J Anaesth 104*, 5 (2010), 538–46. 1

[MV98] MAINTZ J. B., VIERGEVER M. A.: A survey of medical image registration. *Med Image Anal 2*, 1 (1998), 1–36. 1

[MvK14] MENCARELLI A., VAN KRANEN S. R.: Deformable image registration for adaptive radiation therapy of head and neck cancer accuracy and precision in the presence of tumor changes. *Int J Radiat Oncol Biol Phys 90*, 3 (2014), 680–7. 3, 5

[OT14] OLIVEIRA F. P., TAVARES J. M.: Medical image registration: a review. *Comput Methods Biomech Biomed Engin 17*, 2 (2014), 73–93. 1

[RCC15] RIVAZ H., CHEN S. J., COLLINS D. L.: Automatic deformable MR-ultrasound registration for image-guided neurosurgery. *IEEE Trans Med Imaging 34*, 2 (2015), 366–80. 3, 5

[Roh00] ROHR K.: Elastic registration of multimodal medical images: a survey. *Kunstliche Intelligenz* (2000), 11–17. 1

[SBCea08] SOHN M., BIRKNER M., CHI Y., ET AL.: Model-independent, multimodality deformable image registration by local matching of anatomical features and minimization of elastic energy. *Med Phys 35* (2008), 866–78. 4

[SBLD15] SERRURIER A., BONSCH A., LAU R., DESERNO T. M.: MRI visualisation by digitally reconstructed radiographs. *Proc SPIE* (2015), in press. 6

[SD13] SANDOVAL Z. L., DILLENSEGER J.-L.: Evaluation of computed tomography to ultrasound 2D image registration for atrial fibrillation treatment. *Comput Cardiol 40* (2013), 245–48. 3, 4

[SLS*09] SCHEYS L., LOECKX D., SPAEPEN A., SUETENS P., JONKERS I.: Atlas based non rigid image registration to automatically define line of action muscle models a validation study. *J Biomech 42*, 5 (2009), 565–72. 2, 3

[Spi14] SPINCZYK D.: Image based guidance of percutaneous abdomen intervention based on markers for semi automatic rigid registration. *Wideochir Inne Tech Malo Inwazyjne 9*, 4 (2014), 531–6. 3, 5

[TMB12] TASSANI S., MATSOPOULOS G. K., BARUFFALDI F.: 3D identification of trabecular bone fracture zone using an automatic image registration scheme a validation study. *J Biomech 45*, 11 (2012), 2035–40. 3, 4

[UNS*13] UNERI A., NITHIANANTHAN S., SCHAFER S., OTAKE Y., STAYMAN J. W., KLEINSZIG G., SUSSMAN M. S., PRINCE J. L., SIEWERDSEN J. H.: Deformable registration of the inflated and deflated lung in cone beam CT guided thoracic surgery. *Med Phys 40*, 1 (2013), 017501. 1, 3, 4

[YAHF11] YANG X., AKBARI H., HALIG L., FEI B.: 3D non-rigid registration using surface and local salient features for transrectal ultrasound image-guided prostate biopsy. *Proc SPIE Int Soc Opt Eng 1* (2011), 7964–79642V. 1, 3, 4

[ZF03] ZITOVA B., FLUSSER J.: Image registration methods: a survey. *Image Vis Comput 21* (2003), 977–1000. 1

[ZFF*13] ZAMBRANO V., FURTADO H., FABRI D., LUTGENDORF-CAUCIQ C., GORA J., STOCK M., MAYER R., BIRKFELLNER W., GEORG D.: Performance validation of deformable image registration in the pelvic region. *J Radiat Res 54* (2013), i120–8. 3, 4

[zyg] Zygote. http://www.zygote.com. 5

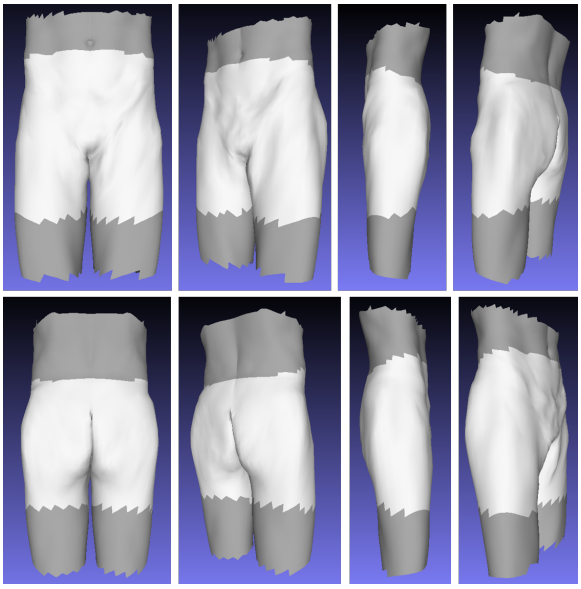

Figure 2: *Final registration regarding the skin for a male subject-specific model.*

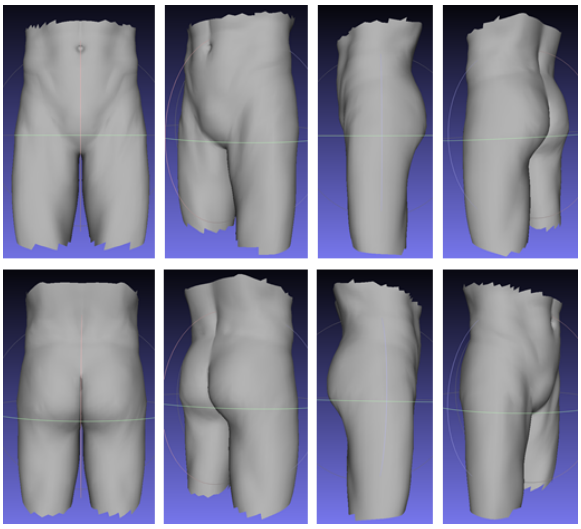

Figure 3: *Zygote male model regarding the skin.*

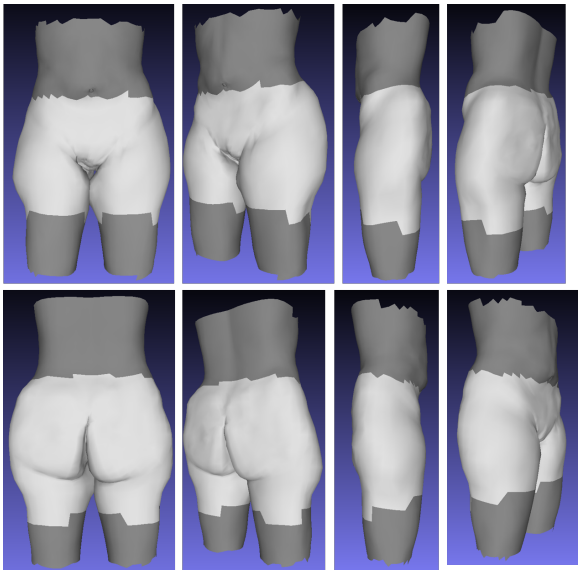

Figure 4: *Final registration regarding the skin for a female subject-specific model.*

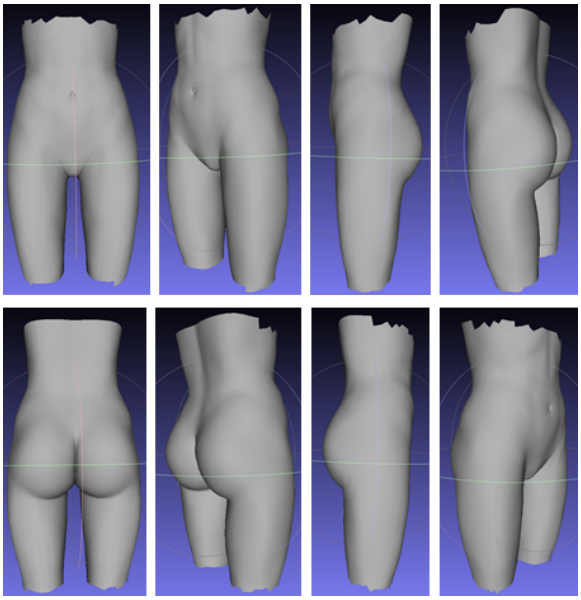

Figure 5: *Zygote female model regarding the skin.*